Spin reorientation in $Ba_{0.65}Na_{0.35}Fe_2As_2$ studied by single-crystal neutron diffraction

F. Waßer,[1] A. Schneidewind,[2] Y. Sidis,[3] S. Wurmehl,[4,5] S. Aswartham,[4] B. Büchner,[4,5] and M. Braden[1,*]

[1]*II. Physikalisches Institut, Universität zu Köln, Zülpicher Straße 77, D-50937 Köln, Germany*
[2]*Jülich Centre for Neutron Science, Forschungszentrum Jülich GmbH, Outstation at MLZ, Lichtenbergstraße 1, D-85748 Garching, Germany*
[3]*Laboratoire Léon Brillouin, CEA/CNRS, F-91191 Gif-sur-Yvette Cedex, France*
[4]*Leibniz-Institut für Festkörper- und Werkstoffforschung Dresden, Helmholtzstraße 20, D-01069 Dresden, Germany*
[5]*Institut für Festkörperphysik, Technische Universität Dresden, D-01171 Dresden, Germany*

We have studied the magnetic ordering in $Ba_{1-x}Na_xFe_2As_2$ with $0.25 \leqslant x \leqslant 0.4$ by unpolarized and polarized neutron diffraction using single crystals. Unlike most FeAs-based compounds that magnetically order, Na-doped $BaFe_2As_2$ exhibits two successive magnetic transitions: For $x = 0.35$, upon cooling, magnetic order occurs at $\sim$70 K with in-plane magnetic moments being arranged as in pure or Ni-, Co-, or K-doped $BaFe_2As_2$ samples. At a temperature of $\sim$46 K a second phase transition occurs, which the single-crystal neutron-diffraction experiments can unambiguously identify as a spin reorientation. At low temperatures, the ordered magnetic moments in $Ba_{0.65}Na_{0.35}Fe_2As_2$ point along the c direction. The two nearly degenerate magnetic states document orbital degeneracy to persist in the superconducting phase.

There are two promising explanations for the appearance of high-temperature superconductivity in FeAs-based materials [1] basing on orbital [2,3] and magnetic fluctuations [4], respectively. Magnetism and orbital degrees of freedom are, however, closely tied in FeAs-based compounds. Although the structural distortion accompanying the antiferromagnetic (AFM) order in the parent materials remains small [5–7], its electronic signatures are rather strong, as seen in the anisotropic resistance [8,9], in angle-resolved photoemission studies (ARPES) [10,11], or optical spectroscopy [12]. This and the fully anisotropic magnon dispersion [13] inspire theoretical models of orbital order driving the magnetic interactions that are similar to those applied to manganites [14–16]. However, the orbital degrees of freedom, which are also essential for nematicity, remain poorly studied by experiment for the metallic FeAs-based compounds.

Here we analyze the spin-space anisotropy arising from spin-orbit coupling (SOC) [17], which constitutes a fingerprint of orbital ordering. Most AFM FeAs-based compounds exhibit a single [18] magnetic transition to a magnetic structure where moments are aligned parallel to the in-plane component of the magnetic propagation vector, which is (0.5,0.5,1) [19] in the 122 family [5–7] [see Fig. 1(a)]. However, in AFM $BaFe_2As_2$ it costs more energy to rotate the magnetic moment within the planes than perpendicular to them [20], contradicting the simple expectation for a layered magnet. Similar anisotropy clearly persists in the magnetic excitations of superconducting (SC) Co- [21], Ni- [22–24], and K-doped [25,26] $BaFe_2As_2$, documenting the persisting role of orbital degrees in the SC phase.

Very recently a second magnetic transition was reported for Na-doped $BaFe_2As_2$ and interpreted as a microscopic superposition of the two equivalent ordering schemes, with propagation vectors (0.5,0.5,1) and (−0.5,0.5,1), into a two-k structure [27]. We have studied single-crystalline samples of $Ba_{1-x}Na_xFe_2As_2$ with $0.25 \leqslant x \leqslant 0.4$, finding clear evidence

for a reorientation of the spins occurring at intermediate doping at low temperatures. This spin reorientation towards alignment of the magnetic moments parallel to the c direction qualitatively agrees with the anisotropies observed in pure and in doped $BaFe_2As_2$, and implies a nearly degenerate orbital configuration.

Single crystals of $Ba_{1-x}Na_xFe_2As_2$ with $0.25 \leqslant x \leqslant 0.4$ were grown using a self-flux high-temperature solution growth technique. Details of sample growth and characterization can be found in Ref. [28]. In particular, the composition of all crystals was determined by electron microscopy with energy-dispersive x-ray analysis (with a precision of about 1%–2%), and SC transition temperatures were measured with a superconducting quantum interference device (SQUID) magnetometer. Due to the air sensitivity of $Ba_{1-x}Na_xFe_2As_2$, all synthesis and characterization procedures as well as the mounting and orienting of the crystals into the sample cans were done in an Ar glove box (with an oxygen content below 5 ppm). Lattice parameters of the large crystals were determined by neutron diffraction using the 3T1 diffractometer at the Orphée reactor in Saclay ($k_i = 2.66$ Å^{-1}). There are two reports on the phase diagram of $Ba_{1-x}Na_xFe_2As_2$ in the literature [29,30], both based on polycrystalline samples. The lattice constants and magnetic properties determined with our single crystals fit to the results reported by Cortes-Gil *et al.* [30] while there seems to be an offset in the Na content when comparing with the data described by Avci *et al.* [29]. Neutron scattering experiments aiming at the characterization of the magnetic structure as a function of temperature were performed at the PANDA triple-axis spectrometer (Maier-Leibnitz Zentrum, Garching, $k_i = 1.55$ and 2.57 Å^{-1}), and at the 3T1 and 4F1 triple-axis spectrometers (both at the Orphée reactor). On the 4F1 spectrometer we used a neutron beam with $k_i = 2.57$ Å^{-1} polarized by a bender and analyzed the final polarization by a Heusler crystal. We performed a longitudinal polarization analysis by guiding the neutron spins with a set of Helmholtz coils. In all experiments either pyrolithic graphite or Be filters were used to suppress higher order contaminations and crystals were oriented in the [110]/[001] scattering planes.
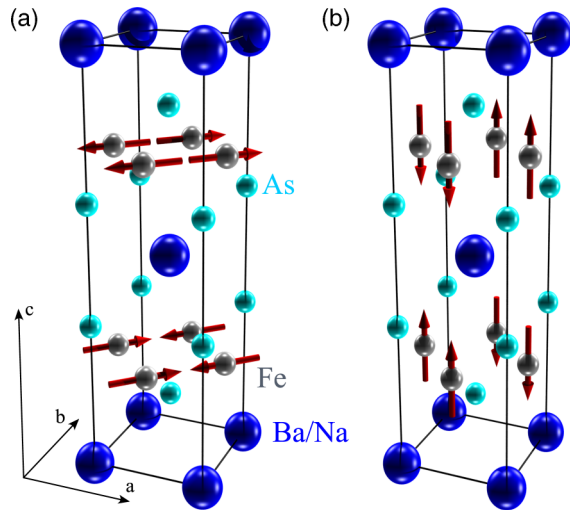
---

*braden@ph2.uni-koeln.de

FIG. 1. (Color online) Magnetic structure of $Ba_{1-x}Na_xFe_2As_2$ in the AFM1 phase $46 < T < 70$ K and in the AFM2 phase at low temperature, $T < 46$ K. Note that the fourfold symmetry axis is broken in both cases by the in-plane component of the magnetic propagation vector chosen as $(0.5, 0.5, 1)$.

FIG. 2. (Color online) (a) Temperature dependence of magnetic and nuclear Bragg reflection intensities in $Ba_{0.65}Na_{0.35}Fe_2As_2$ measured on the PANDA spectrometer. Note that the magnetic, $(0.5,0.5,1)$ and $(0.5,0.5,3)$, and nuclear, (112) and (002), Bragg peaks refer to different scales. (112) and (002) intensities were measured upon heating and cooling, respectively. (b) and (c) show an enlargement of the low-temperature range, illustrating the reduction of magnetic intensities in the SC state.

Figure 1 shows the crystal and the magnetic structures of $Ba_{1-x}Na_xFe_2As_2$. Figure 1(a) corresponds to the alignment of magnetic moments parallel to the layers, which is found in most FeAs-based compounds [5–7]. One has to distinguish three orthogonal directions: One is defined by the in-plane component of the magnetic propagation vector [chosen here as $(0.5,0.5,1)$], $[1,1,0]$ labeled longitudinal in plane, the second is $[-1,1,0]$ transversal in plane, and the third $[0,0,1]$ out of plane. Figure 2 shows the temperature dependence of nuclear and magnetic Bragg reflections measured on single-crystalline $Ba_{0.65}Na_{0.35}Fe_2As_2$, $m = 90$ mg, mosaic spread $\eta = 1.3°$ (full width at half maximum including a resolution of PANDA of about $0.8°$). The magnetic peaks $(0.5,0.5,1)$ and $(0.5,0.5,3)$ start to increase in intensity when cooling below the first magnetic transition at 70 K. There is a second magnetic transition at lower temperature where both peaks increase further, but this low-temperature intensity enhancement is much stronger for the $(0.5,0.5,1)$ Bragg peak. Already this different behavior of the intensities at the two transitions indicates a change in the magnetic structure at the lower transition. Figure 2 also shows the temperature dependence of two nuclear Bragg peaks which both show anomalies at the two magnetic transitions [31]. This impact of the magnetic ordering on the nuclear structure underlines close coupling, but a clear interpretation of these structural effects is not obvious. The emergence of orthorhombic domains in the magnetically ordered phase has a strong impact on the extinction and multiple diffraction conditions of nuclear Bragg reflections [21]. The up and down shifts of the nuclear intensities at the two transitions indicates that the structural changes appearing at the high-temperature magnetic transition get suppressed at the lower transition. The anomalies in the nuclear Bragg peaks are not perfectly sharp, as it can be expected for an extinction effect at a structural transition, but the width of the anomaly amounts only to a few degrees K, so that any local variation of the Na doping must be very limited.
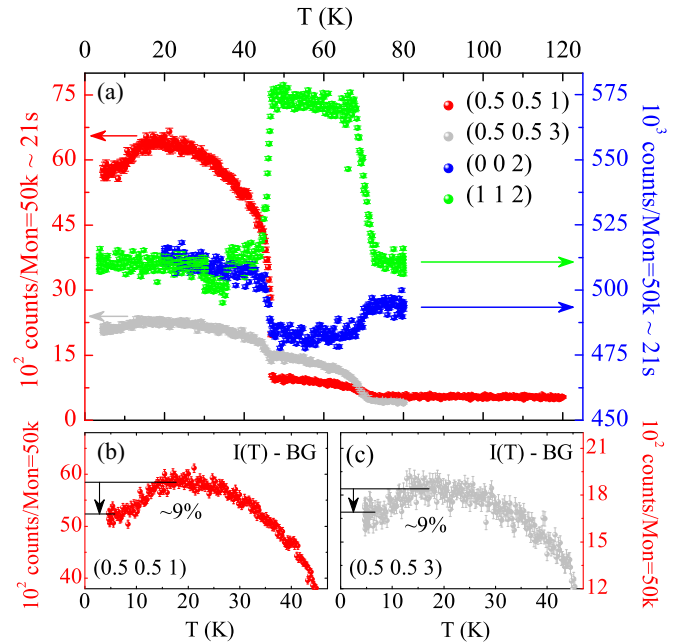
There is a third anomaly visible in the temperature dependencies of the magnetic Bragg peaks. At low temperature in the SC state both magnetic Bragg peaks decrease in intensity (see Fig. 2), although the drop in magnetic intensity seems to occur slightly below $T_c = 26$ K, similar to observations in K-doped $BaFe_2As_2$ [32]. The relative reduction in the two magnetic peaks in $Ba_{0.65}Na_{0.35}Fe_2As_2$ is identical, indicating that this sample exhibits a single magnetic phase at low temperature whose ordered moment gets reduced in the SC state.

In order to quantitatively analyze the change in magnetic structure we have measured integrated intensities on PANDA by performing rocking scans. The integrated intensities were corrected for the Lorentz factor and are traced in Fig. 3 against the q_l component. Neutron diffraction only measures the magnetic moment perpendicular to the scattering vector. Any magnetic diffraction intensity is weighted with a factor $\sin^2(\alpha)$, with α being the angle between the magnetic moment and the scattering vector. By enhancing the q_l component in the magnetic Bragg reflection $\mathbf{Q} = (0.5,0.5,q_l)$, a magnetic moment aligned along the c direction contributes less and a moment along the in-plane component of the Bragg scattering vector, i.e., along $[110]$, contributes more strongly. In addition, the magnetic form factor depends on the length of the scattering vector in an isotropic approximation and reduces the magnetic scattering at larger Q values. Both effects can be calculated for $\mathbf{Q} = (0.5,0.5,q_l)$ and are included in Fig. 3 for the usual magnetic arrangement, with moments aligned along the in-plane component of the propagation vector (orange
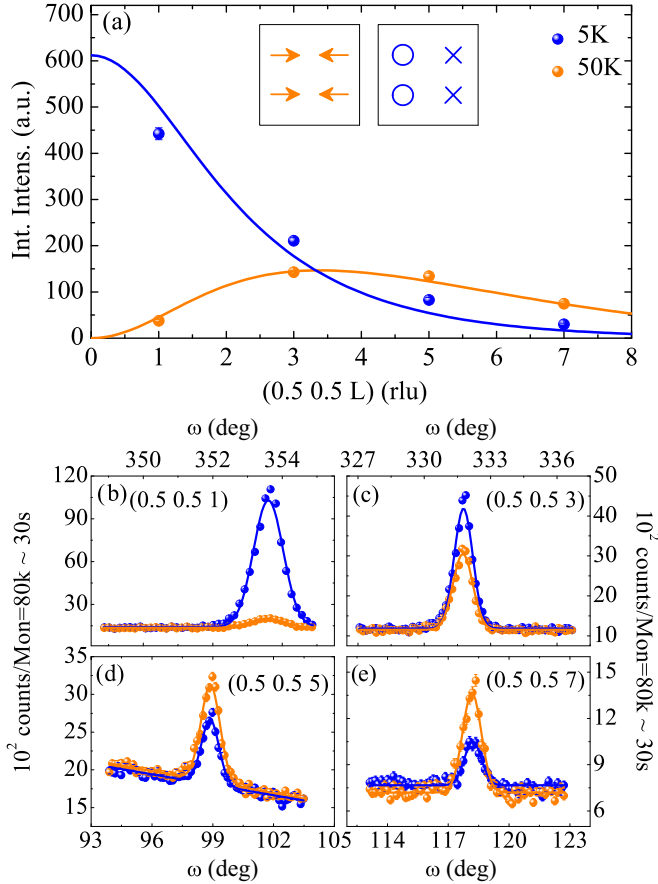
FIG. 3. (Color online) (a) shows the l dependence of magnetic integrated intensities in the AFM1 and AFM2 phases. The lines are model calculations for the magnetic structures shown in Fig. 1 with moments parallel to the a and c directions. (b)–(e) Rocking scans across the magnetic Bragg peaks (0.5,0.5,l) with l = 1, 3, 5, 7, measured on the PANDA spectrometer at 5 and 50 K, in the AFM2 and AFM1 phases, respectively.

line, index a) and for out-of-plane alignment (blue line, index c):

$$I_{a,c}(0.5,0.5,q_l) \propto [f(|Q|)m\sin(\alpha_{a,c})]^2, \qquad (1)$$

$$\sin(\alpha_a) = \frac{q_l\frac{2\pi}{c}}{Q}, \quad \sin(\alpha_c) = \frac{\frac{1}{\sqrt{2}}\frac{2\pi}{a}}{Q}. \qquad (2)$$

At 50 K, i.e., in the magnetic phase at higher temperatures, the integrated intensities are perfectly described by the in-plane arrangement, while the low-temperature data agree well with the out-of-plane alignment. Some minor deviations may arise from an anisotropic magnetic form factor or from a small fraction of the sample staying in the AFM1 phase [fitting the data in Fig. 3(a) with both phases and equal moments indicates only 13% AFM1].

We may conclude that Ba$_{0.65}$Na$_{0.35}$Fe$_2$As$_2$ exhibits a spin reorientation transition at ∼46 K with moments aligned along the c direction at low temperature. The different intensity changes observed at different (0.5,0.5,q_l) peaks are furthermore illustrated in the lower parts of Fig. 3. The gain in intensity is most pronounced at (0.5,0.5,1), where
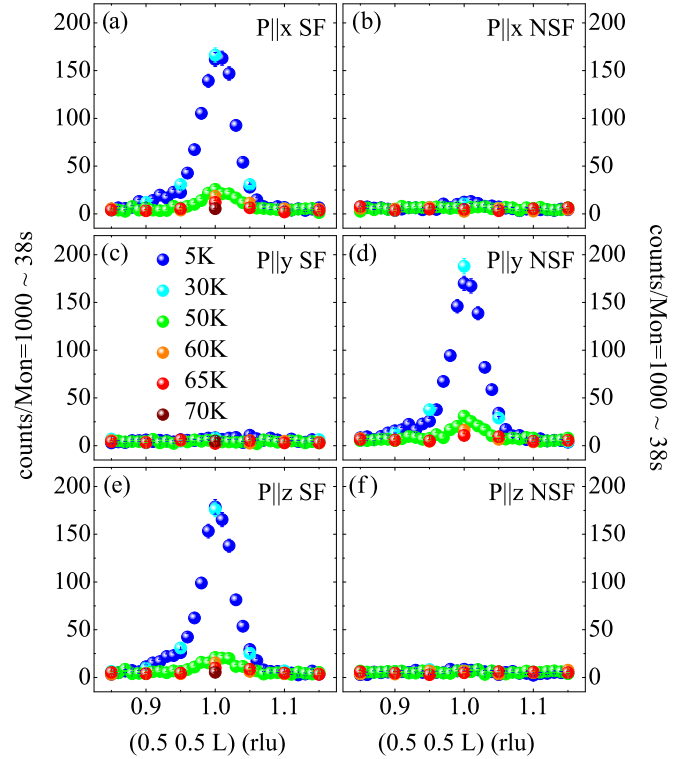

FIG. 4. (Color online) Results of polarized neutron-diffraction experiments on the 4F spectrometer. Scans were performed across the (0.5,0.5,1) magnetic Bragg peak in both the SF and NSF channel for the neutron polarization along the x, y, and z directions. There is no indication of any scattering associated with a magnetic moment pointing in the [1, −1,0] direction.

the geometry factor strongly hampers the observation of the magnetic peaks in the AFM1 phase, $\sin^2(\alpha_a) = 0.16$, while out-of-plane moments contribute with an almost full geometry factor in AFM2, $\sin^2(\alpha_c) = 0.84$. The scans across (0.5,0.5,5) and (0.5,0.5,7) show that these intensities even decrease at the lower transition because the geometry factor is strongly reduced at the spin reorientation.

We have strengthened our conclusion about the spin reorientation in Ba$_{0.65}$Na$_{0.35}$Fe$_2$As$_2$ by experiments using polarized neutron scattering (see Fig. 4). The sample was again mounted with the [110]/[001] scattering plane. The polarization analysis adds the additional selection rule that magnetic scattering contributes to the spin-flip (SF) signal if the magnetic contribution is perpendicular to the axis of the polarization analysis, while the component parallel to the polarization axis contributes to the non-spin-flip (NSF) scattering. One may analyze the SF and NSF signals for setting the neutron-polarization axis parallel to the scattering vector (labeled the x direction), parallel to the [$\bar{1}$10] direction (labeled the z direction, as it is perpendicular to the scattering plane), and perpendicular to these two directions (labeled the y direction). Figure 4 shows the measurement obtained with the Ba$_{0.65}$Na$_{0.35}$Fe$_2$As$_2$ crystal at the (0.5,0.5,1) reflection, with measurements at (0.5,0.5,3) yielding the same results [31]. For the x-axis polarization analysis the scattering appears almost entirely in the SF channel, as it is expected for a magnetic signal. The small leakage in the NSF channel is due

to imperfections of the polarization analysis, but note that the flipping ratio of the total experimental setup is quite high, ∼31. Concerning the other two polarization directions, the signal is entirely found in the NSF channel in the y direction and in the SF channel in the z direction. These findings document that there is no ordered magnetic moment along the [$\bar{1}$10] direction (in-plane transversal) either in the high-temperature or in the low-temperature phase. The magnetic structure with the same propagation vector (0.5,0.5,1) but with transversal in-plane moments is not observed in $Ba_{0.65}Na_{0.35}Fe_2As_2$. The magnetic moment thus always stays within the scattering plane. Taking into account the q_l dependence of the signal, the spin reorientation from the [110] to [001] directions is the only possible explanation of our single-crystal data.

At the 3T1 diffractometer, we have also studied another crystal with a 35% Na doping ($m = 210$ mg, $\eta = 0.6°$) as well as ones with 25% ($m = 66$ mg, $\eta = 2.2°$) and 39% ($m = 172$ mg, $\eta = 0.8°$). All these crystals qualitatively show the same two magnetic transitions and the spin reorientation. However, the transition temperatures depend on the doping (25% Na: $T_C = 5$, $T_{N1} = 120$, and $T_{N2} = 35$ K; 39% Na: $T_C = 29$, $T_{N1} = 61$, and $T_{N2} = 44.5$ K), and for 25% and 39% Na contents the low-temperature phase transition seems to remain incomplete, indicating the limits of the stability of the c-aligned magnetic phase. A crystal with a doping content of 40% ($m = 42$ mg, $\eta = 0.8°$ at 3T1) did not show any static magnetic ordering, indicating a rapid suppression of the magnetic phase.

Avci *et al.* reported on powder neutron-diffraction experiments on a sample with a nominal composition $Ba_{0.76}Na_{0.24}Fe_2As_2$ [27] which also indicate a second magnetic transition, in good agreement with our results. This powder sample shows reentrance into an almost tetragonal phase, but the powder data and the fact that 40% of the sample did not transform prohibited an unambiguous determination of the magnetic structure. The results in Ref. [27] were discussed as evidence for a $2k$ magnetic structure associated with the simultaneous condensation of both nematic order parameters. Since our results clearly document the spin reorientation as the main element of the low-temperature magnetic transition, the possible existence of a $2k$ structure needs further analysis, because such a structure implies nonmagnetic or weakly magnetic sites for c-aligned moments, and because the spin reorientation can at least partially explain the suppression of the orthorhombic splitting. Our data further document that nematic aspects are not driving the low-temperature magnetic transition in $Ba_{1-x}Na_xFe_2As_2$.

The spin reorientation in $Ba_{1-x}Na_xFe_2As_2$ agrees qualitatively with the anisotropy of magnetic excitations in pure $BaFe_2As_2$ [20], where rotating the moment into the c direction corresponds to the lower anisotropy energy, in contrast to the expectation for a layered magnet. Na substitution seems to further reduce the c-axis anisotropy energy so that it becomes the ground state order at $x = 0.35$. The change in the direction of the magnetic moment must be associated with a slightly different orbital arrangement.

The ARPES experiments in the AFM phase of $BaFe_2As_2$ indicate significant lowering of the electronic band associated with d_{xz} orbitals (in the coordinates with a along the AFM ordered moment) [10]. In a simple localized picture, orbital

ordering with enhanced occupation of the d_{xz} orbital can mix through SOC with other orbitals, yielding a finite orbital moment. Linear combinations with the other t_{2g} orbitals $d_{xz} + id_{yz}$ and $d_{xz} + id_{xy}$ yield orbital moments along z and x, respectively, which are the two directions of ordered moments in AFM FeAs materials. The enhanced occupation of the d_{xz} orbital observed in ARPES qualitatively agrees with the observed ground states in the two AFM phases, but a quantitative analysis of the SOC in the metallic AFM state is highly desirable. Avci *et al.* [29] find that the FeAs layers are more extended in the c direction in the Na-doped series, which favors the orientation of magnetic moments in the c direction, giving further support to our orbital physics argumentation. The two different magnetic arrangements appearing in FeAs compounds, furthermore, indicate that the magnetic character in these materials is not Ising like; orbital effects imply a magnetic hard axis (transversal in plane).

The c-polarized phase agrees with the observation of an additional low-energy resonance mode in optimally Co-doped $BaFe_2As_2$, which appeared in the c-polarized channel [21]. Similar experiments on Ni- [24] and K-doped [25,26] $BaFe_2As_2$ added that the low-energy mode also has a longitudinal in-plane character. Therefore, one may conclude that doped SC $BaFe_2As_2$ exhibits the lowest magnetic excitations in the in-plane longitudinal and in the c-oriented channels (easy plane) while in-plane transversal (hard-axis) excitations lie higher in energy. The low-energy excitations in the SC samples thus correspond to the two directions, where static ordered moments are observed. The easy-plane anisotropy is thus relevant in the entire phase diagram of FeAs-based materials. The two almost degenerate magnetic orientations further indicate that orbital degeneracy remains sizable deep in the SC phase.

So far only $Ba_{1-x}Na_xFe_2As_2$ exhibits the c-polarized order, but the high-pressure phase recently reported in K-doped $BaFe_2As_2$ [33] as well as low-temperature structures in REFeAsO [18] could possess the same character. Magnetic order in the transversal in-plane direction is not observed, reflecting the fact that the corresponding magnetic response in the SC compounds lies always higher in energy [21–26].

In conclusion, we have shown that $Ba_{1-x}Na_xFe_2As_2$ close to the suppression of AFM ordering, i.e., for $0.25 \leqslant x \leqslant 0.39$, exhibits a spin reorientation at low temperatures. The magnetic order in $Ba_{0.65}Na_{0.35}Fe_2As_2$ corresponds to that observed in most other FeAs-based magnetic materials for temperatures between 46 and 70 K, but at 46 K the magnetic moments reorient along the c direction. The two almost degenerate magnetic spin configurations imply that orbital degeneracy persists well into the SC phase. AFM and SC FeAs-based compounds exhibit evidence for the same and sizable easy-plane anisotropy, underlining the importance of taking SOC and orbital aspects into account.

[1] Y. Kamihara, T. Watanabe, M. Hirano, and H. Hosono, J. Am. Chem. Soc. **130**, 3296 (2008).

[2] H. Kontani and S. Onari, Phys. Rev. Lett. **104**, 157001 (2010).

[3] S. Onari and H. Kontani, Phys. Rev. Lett. **109**, 137001 (2012).

[4] P. J. Hirschfeld, M. M. Korshunov, and I. I. Mazin, Rep. Prog. Phys. **74**, 124508 (2011).

[5] C. de la Cruz, Q. Huang, J. W. Lynn, J. Li, W. Ratcliff, J. L. Zarestky, H. A. Mook, G. F. Chen, J. L. Luo, N. L. Wang, and P. Dai, Nature (London) **453**, 899 (2008).

[6] Q. Huang, Y. Qiu, Wei Bao, M. A. Green, J. W. Lynn, Y. C. Gasparovic, T. Wu, G. Wu, and X. H. Chen, Phys. Rev. Lett. **101**, 257003 (2008).

[7] N. Qureshi, Y. Drees, J. Werner, S. Wurmehl, C. Hess, R. Klingeler, B. Büchner, M. T. Fernandez-Díaz, and M. Braden, Phys. Rev. B **82**, 184521 (2010).

[8] J. H. Chu, J. G. Analytis, K. De Greve, P. L. McMahon, Z. Islam, Y. Yamamoto, and I. R. Fisher, Science **329**, 824 (2010).

[9] T.-M. Chuang, M. P. Allan, J. Lee, Y. Xie, Ni Ni, S. L. Bud'ko, G. S. Boebinger, P. C. Canfield, and J. C. Davis, Science **327**, 181 (2010).

[10] M. Yi, D. Lu, J.-H. Chu, J. G. Analytis, A. P. Sorini, A. F. Kemper, B. Moritz, S.-K. Mo, R. G. Moore, M. Hashimoto, W.-S. Lee, Z. Hussain, T. P. Devereaux, I. R. Fisher, and Z.-X. Shen, Proc. Natl. Acad. Sci. U.S.A. **108**, 6878 (2011).

[11] T. Shimojima, K. Ishizaka, Y. Ishida, N. Katayama, K. Ohgushi, T. Kiss, M. Okawa, T. Togashi, X.-Y. Wang, C.-T. Chen, S. Watanabe, R. Kadota, T. Oguchi, A. Chainani, and S. Shin, Phys. Rev. Lett. **104**, 057002 (2010).

[12] M. Nakajima, T. Liang, S. Ishida, Y. Tomioka, K. Kihou, C. H. Lee, A. Iyo, H. Eisaki, T. Kakeshita, T. Ito, and S. Uchida, Proc. Natl. Acad. Sci. U.S.A. **108**, 12238 (2011).

[13] L. W. Harriger, H. Q. Luo, M. S. Liu, C. Frost, J. P. Hu, M. R. Norman, and P. Dai, Phys. Rev. B **84**, 054544 (2011).

[14] F. Krüger, S. Kumar, J. Zaanen, and J. van den Brink, Phys. Rev. B **79**, 054504 (2009).

[15] C.-C. Lee, W.-G. Yin, and W. Ku, Phys. Rev. Lett. **103**, 267001 (2009).

[16] W. Lv and P. Phillips, Phys. Rev. B **84**, 174512 (2011).

[17] It is well known that spin-space anisotropy results either from magnetic dipolar interactions, which can be neglected here, or relativistic spin-orbit coupling [see J. Kanamori in *Magnetism I*, edited by G. T. Rado and H. Suhl (Academic, New York, 1963)].

[18] Only for *RE*FeAsO, with *RE* a magnetic rare earth, are additional transitions reported associated with the ordering of the *RE*

moments; above this *RE* ordering no spin reorientation of Fe moments occurs; H. Maeter *et al.*, Phys. Rev. B **80**, 094524 (2009).

[19] We use reduced lattice units with respect to $\frac{2\pi}{a}$ and $\frac{2\pi}{c}$ with $a \sim 3.9$ and $c \sim 13.1$ Å.

[20] N. Qureshi, P. Steffens, S. Wurmehl, S. Aswartham, B. Büchner, and M. Braden, Phys. Rev. B **86**, 060410 (2012).

[21] P. Steffens, C. H. Lee, N. Qureshi, K. Kihou, A. Iyo, H. Eisaki, and M. Braden, Phys. Rev. Lett. **110**, 137001 (2013).

[22] O. J. Lipscombe, L. W. Harriger, P. G. Freeman, M. Enderle, C. Zhang, M. Wang, T. Egami, J. Hu, T. Xiang, M. R. Norman, and P. Dai, Phys. Rev. B **82**, 064515 (2010).

[23] M. Liu, C. Lester, J. Kulda, X. Lu, H. Luo, M. Wang, S. M. Hayden, and P. Dai, Phys. Rev. B **85**, 214516 (2012).

[24] H. Luo, M. Wang, C. Zhang, X. Lu, L.-P. Regnault, R. Zhang, S. Li, J. Hu, and P. Dai, Phys. Rev. Lett. **111**, 107006 (2013).

[25] C. Zhang, M. Liu, Y. Su, L.-P. Regnault, M. Wang, G. Tan, T. Brückel, T. Egami, and P. Dai, Phys. Rev. B **87**, 081101(R) (2013).

[26] N. Qureshi, C. H. Lee, K. Kihou, K. Schmalzl, P. Steffens, and M. Braden, Phys. Rev. B **90**, 100502(R) (2014).

[27] S. Avci, O. Chmaissem, S. Rosenkranz, J. M. Allred, I. Eremin, A. V. Chubukov, D. E. Bugaris, D. Y. Chung, M. G. Kanatzidis, J.-P. Castellan, J. A. Schlueter, H. Claus, D. D. Khalyavin, P. Manuel, A. Daoud-Aladine, and R. Osborn, Nat. Commun. **5**, 3845 (2014).

[28] S. Aswartham, M. Abdel-Hafiez, D. Bombor, M. Kumar, A. U. B. Wolter, C. Hess, D. V. Evtushinsky, V. B. Zabolotnyy, A. A. Kordyuk, T. K. Kim, S. V. Borisenko, G. Behr, B. Büchner, and S. Wurmehl, Phys. Rev. B **85**, 224520 (2012).

[29] S. Avci, J. M. Allred, O. Chmaissem, D. Y. Chung, S. Rosenkranz, J. A. Schlueter, H. Claus, A. Daoud-Aladine, D. D. Khalyavin, P. Manuel, A. Llobet, M. R. Suchomel, M. G. Kanatzidis, and R. Osborn, Phys. Rev. B **88**, 094510 (2013).

[30] R. Cortes-Gil, D. R. Parker, M. J. Pitcher, J. Hadermann, and S. J. Clarke, Chem. Mater. **22**, 4304 (2010).

[31] See Supplemental Material at http://link.aps.org/supplemental/10.1103/PhysRevB.91.060505 for additional information on the experiments.

[32] E. Wiesenmayer, H. Luetkens, G. Pascua, R. Khasanov, A. Amato, H. Potts, B. Banusch, H.-H. Klauss, and D. Johrendt, Phys. Rev. Lett. **107**, 237001 (2011).

[33] E. Hassinger, G. Gredat, F. Valade, S. R. de Cotret, A. Juneau-Fecteau, J.-Ph. Reid, H. Kim, M. A. Tanatar, R. Prozorov, B. Shen, H.-H. Wen, N. Doiron-Leyraud, and L. Taillefer, Phys. Rev. B **86**, 140502(R) (2012).